
Article:
Procacci, Barbara orcid.org/0000-0001-7044-0560, Aguiar, Pedro M., Halse, Meghan Eileen orcid.org/0000-0002-3605-5551 et al. (2 more authors) (2016) Photochemical Pump and NMR Probe to monitor the formation and kinetics of hyperpolarized metal dihydrides. Chemical Science. SC-EDG-05-2016-001956.R1. pp. 7087-7093. ISSN 2041-6539

https://doi.org/10.1039/C6SC01956K

Chemical Science

EDGE ARTICLE

View Article Online
View Journal | View Issue

Cite this: *Chem. Sci.*, 2016, **7**, 7087

Photochemical pump and NMR probe to monitor the formation and kinetics of hyperpolarized metal dihydrides†

Barbara Procacci,[ab] Pedro M. Aguiar,[b] Meghan E. Halse,[ab] Robin N. Perutz*[b] and Simon B. Duckett*[ab]

On reaction of $IrI(CO)(PPh_3)_2$ **1** with para-hydrogen (p-H_2), $Ir(H)_2I(CO)(PPh_3)_2$ **2** is formed which exhibits strongly enhanced ^1H NMR signals for its hydride resonances. Complex **2** also shows similar enhancement of its NMR spectra when it is irradiated under p-H_2. We report the use of this photochemical reactivity to measure the kinetics of H_2 addition by laser-synchronized reactions in conjunction with NMR. The single laser pulse promotes the reductive elimination of H_2 from $Ir(H)_2I(CO)(PPh_3)_2$ **2** in C_6D_6 solution to form the 16-electron precursor **1**, back reaction with p-H_2 then reforms **2** in a well-defined nuclear spin-state. The build up of this product can be followed by incrementing a precisely controlled delay (τ), in millisecond steps, between the laser and the NMR pulse. The resulting signal *vs.* time profile shows a dependence on p-H_2 pressure. The plot of k_{obs} against p-H_2 pressure is linear and yields the second order rate constant, k_2, for H_2 addition to **1** of $(3.26 \pm 0.42) \times 10^2$ M^{-1} s^{-1}. Validation was achieved by transient-UV-vis absorption spectroscopy which gives k_2 of $(3.06 \pm 0.40) \times 10^2$ M^{-1} s^{-1}. Furthermore, irradiation of a C_6D_6 solution of **2** with multiple laser shots, in conjunction with p-H_2 derived hyperpolarization, allows the detection and characterisation of two minor reaction products, **2a** and **3**, which are produced in such low yields that they are not detected without hyperpolarization. Complex **2a** is a configurational isomer of **2**, while **3** is formed by substitution of CO by PPh_3.

Received 4th May 2016
Accepted 3rd August 2016

DOI: 10.1039/c6sc01956k

www.rsc.org/chemicalscience

Introduction

A number of pump-probe time-resolved techniques have been developed that allow chemical reactions that happen on extremely fast timescales (milliseconds down to femtoseconds) to be followed and understood. Whilst various probe methods have been successfully exploited,[1–4] the level of structurally diagnostic information available is often limited compared to that provided by nuclear magnetic resonance (NMR). Therefore, the corresponding time-resolved NMR spectroscopy method would be a very powerful analytical tool capable of providing complementary structural and kinetic information. The existing sensitivity limitation of NMR spectroscopy would, however, need to be overcome in order to achieve this aim. *para*-Hydrogen (p-H_2) induced polarization (PHIP) provides the necessary increase in sensitivity and the benefit of enhancement of resonances that often allow structure determination.[5,6]

We recently described a laser pump-NMR probe technique in which the laser initiation of a reaction is synchronized to NMR detection, such that NMR spectra can be recorded at well-defined intervals after a laser pulse (Fig. 1). In this method, p-H_2 hyperpolarization[5,6] enhances the sensitivity of the NMR detection method so much that the dihydride complexes can be observed in optically dilute solutions with a single NMR scan at intervals as short as 10 μs after the laser pulse. When dihydrogen addition is very fast, the magnetisation that is created through the use of p-H_2 evolves coherently during the well-defined interval τ such that sinusoidal oscillations can subsequently be detected through radio frequency excitation. These oscillations have periods corresponding to the frequency difference between the inequivalent hydrides and/or their difference in spin–spin coupling to a heteronucleus such as phosphorus.[7] Notably, the laser method generates the hyperpolarized molecules synchronously unlike the usual PHIP methods which are inherently asynchronous.[8,9] We now wish to validate the method for the measurement of chemical reaction kinetics on timescales where these initial oscillations are dephased, but short enough that substantial *para*-hydrogen-induced-polarization (PHIP) is retained despite the effects of

[a]*Centre for Hyperpolarisation in Magnetic Resonance, Department of Chemistry, York Science Park, University of York, Heslington, York, YO10 5NY, UK. E-mail: simon.duckett@york.ac.uk*

[b]*Department of Chemistry, University of York, Heslington, York YO10 5DD, UK. E-mail: robin.perutz@york.ac.uk*

† Electronic supplementary information (ESI) available: Experimental details; synthesis and characterisation of compounds, photochemical experiments, kinetic data, UV-vis data. See DOI: 10.1039/c6sc01956k

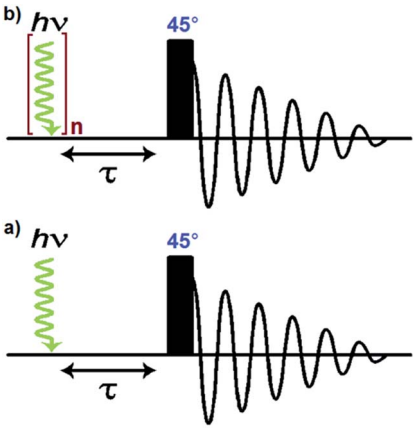

Fig. 1 Pulse sequences used in the laser pump-NMR probe experiments. (a) In the single-shot experiments, a single laser pulse (5 ns) is followed by a delay (τ) for evolution of the chemical system before observation is achieved through the application of a 45° RF pulse. (b) The multiple laser pulse experiments apply a train of laser pulses, separated by an additional delay of 100 ms between each of the n pulses.

relaxation. The method we illustrate involves a degenerate reaction, where H_2 is photodissociated from the parent and *p*-H_2 adds to reform the same molecule but now in a defined nuclear spin state (indicated by asterisk, eqn (1)). In our experiments, *p*-H_2 addition occurs in the high magnetic field of the spectrometer, a situation sometimes referred to as PASADENA conditions.[5,8]

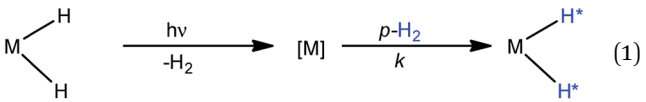

(1)

In order to validate the proposed kinetic measurements, the rate of reaction of the intermediate [M] with H_2 must be known already (or be capable of independent measurement) and ideally have a pseudo first-order rate constant of *ca.* 0.1 to 10 s^{-1} at 3 bar H_2 to satisfy the NMR criteria above. The thermal reactions of these complexes with *p*-H_2 should also be understood. For this purpose, we selected $Ir(H)_2I(CO)(PPh_3)_2$ **2**, derived from the iodide analogue of Vaska's complex, $IrI(CO)(PPh_3)_2$ **1**, for which kinetic data for reaction with dihydrogen[10–12] and underlying reactivity are known.[13–15] Complex **2** can be readily prepared by thermal reaction of the d^8 square-planar precursor $IrI(CO)(PPh_3)_2$ **1** with H_2 in C_6D_6 solution.[16]

The steady state photochemistry of $Ir(H)_2X(CO)(PPh_3)_2$ (X = Cl, I) complexes has been reported (366 nm, C_6H_6) previously and shown to access their Ir(I) counterparts by reductive elimination of H_2, which then undergo oxidative addition of H_2 to reform the parent dihydride.[15] In this context, the photochemical reductive elimination step allows access to its thermal microscopic reverse, oxidative addition, in a controlled way. While time-resolved spectroscopy has been used to examine these chloride complexes, the literature is not definitive on the primary photo-process. Measurements by time resolved UV-vis spectroscopy on solutions of $IrCl(CO)(PPh_3)_2$ and $IrCl(H)_2(CO)(PPh_3)_2$ (λ_{exc} > 254 nm, flash lamp) suggest CO photodissociation as a primary step[17] while time resolved IR spectroscopy (λ_{exc} = 308 nm, laser) excludes any loss of CO on the basis of a lack of evidence for the bleaching of the parent CO stretch.[18] Both studies detected a short-lived transient (~10 μs) which was speculated to be a dimeric species. Studies on the thermal addition of *p*-H_2 to a series of related complexes, ($IrCl(CO)(PPh_3)_2$ and $RhCl(CO)(PPh_3)_2$) have been previously reported.[19,20] These experiments yielded large PHIP enhancements for the iridium and rhodium dihydride products visible for tens of minutes, hence demonstrating the reversibility of H_2 addition and permitting signal averaging. Using both theoretical and experimental approaches, Bargon assessed the purity of the singlet state that is created between the hydride ligands of $IrCl(H)_2(CO)(PPh_3)_2$ upon the addition of *p*-H_2 as greater than 50%.[21] In the case of $IrCl(CO)(PPh_3)_2$, thermal reaction studies demonstrated that a minor *cis–cis* isomer of $IrCl(H)_2(CO)(PPh_3)_2$ can be detected in addition to the more usual *trans–cis* product.[22,23] In contrast, for derivatives of $RhCl(CO)(PPh_3)_2$, a series of binuclear products were detected which contain either bridging or terminal hydride or halide ligands. These products were proposed to form *via* CO loss from $M(H)_2X(CO)(PPh_3)_2$ [X = halide] with the result that a 16-electron $M(H)_2X(PPh_3)_2$ species is created. The presence of this intermediate was confirmed by trapping with added phosphine in a series of experiments which revealed that $IrCl(H)_2(PPh_3)_2$ exhibits a square pyramidal geometry.[20] Furthermore, extensive studies on IrX(CO)(dppe) have been reported establishing that dihydrogen adds to these complexes in a stereoselective way controlled by the X and the CO ligands.[24]

In this work, we report the investigation of the thermal and photochemical reactions of $IrI(CO)(PPh_3)_2$ **1** and $Ir(H)_2I(CO)(PPh_3)_2$ **2** in the presence of *p*-H_2. We use our laser pump-NMR probe method to determine the kinetics of reaction of **2** with H_2 and compare with the results of laser flash photolysis with UV-vis detection.

Experimental‡

Complex **1** was prepared using the procedure reported in the literature.[10] Complex **2** was obtained by hydrogenation of **1** at 50 °C and complete conversion to the 18-electron dihydride was established from NMR spectra recorded at 298 K. *p*-H_2 was generated by cooling hydrogen gas over charcoal in a copper block at 26 K. The proportion of *p*-H_2 at 26 K was calculated as >99%. Pressures of *p*-H_2 were measured with an MKS Baratron capacitance manometer. All NMR spectra were recorded on a Bruker Avance II 600 MHz spectrometer with a 14 T widebore magnet fitted with a 5 mm BBO probe. *In situ* laser photolysis was carried out with a pulsed Nd:YAG laser (Continuum Surelite II) fitted with a frequency tripling crystal (output 355 nm). Operating conditions were typically: 10 Hz repetition rate, flash lamp voltage 1.49 kV, and Q-switch delay increased from the standard to 320 μs yielding a laser power of 75 mW in internal mode. The energy of a single laser pulse was measured using an energy meter calibrated for 355 nm to be ~29.8 mJ at our

operating conditions (external triggering with Q-switch delay set to 150 μs). The unfocused laser beam is directed at the base of the spectrometer and reflected up into the probe *via* a mirror as previously reported.[7] Adjustment screws control the vertical and horizontal position of the mirror which is on a kinematic mount. The system is fully shielded from the operator and the screws of the kinematic mount can be adjusted remotely. The laser radiation is incident on a fixed mirror that is level with the sample and passes through a hole in the probe onto the NMR tube. Standard NMR tubes fitted with Young's taps were used. The samples contained 1–2 mg of compound ($Abs_{355} \sim 0.7$) and approximately 0.4 mL of solvent. A sample of $Ru(dppe)_2H_2$ in C_6D_6 was used for laser alignment with *p*-H_2 amplification in real time. Standard NMR pulse sequences were modified for use with *p*-H_2 by including a synchronized laser initiation sequence prior to NMR excitation. A purpose-written program was used to control the laser firing from the NMR console with the laser set on external triggering. The program sets the laser to fire one warm-up shot before the fire signal. The NMR pulse is initiated at a set delay time (τ) following the fire signal. The intrinsic time delay between sending the fire signal from the spectrometer and the actual firing of the laser pulse was measured with a photodiode and an oscilloscope to be 150 μs (equal to the Q-switch delay for the generation of the pulse). This signal delay was incorporated into the pulse sequence such that synchronized measurements with a time delay, τ, were achieved by setting the spectrometer delay to: τ + 150 μs. The precision of this delay between the laser and radio frequency (RF) pulses is controlled by the 200 ns clock of the spectrometer.

The samples for laser flash photolysis (LFP) were prepared exclusively in a nitrogen glove box. It was loaded into a quartz cuvette (10 mm path-length) fitted with a J-Young's PTFE stopcock, a degassing bulb, and a greaseless Young's connection. The complex was dissolved in benzene (5 mL) with a concentration selected to have an absorbance at the laser wavelength (355 nm) between 0.6 and 0.85. The solution was then degassed by repeated freeze–pump–thaw cycles (3 times) on a high-vacuum Schlenk line before being backfilled with hydrogen. For high pressure work the window edges of the cuvette were flamed to secure the seal and the Young's connection was replaced by a glass-to-metal seal and a Swagelok™ fitting. The gas was admitted on a high pressure line and the pressure measured with an MKS Baratron capacitance manometer. The cell was held in a metal container for safety. A single sample was used for each run with increasing gas pressure. Hydrogen was of Research Grade N5.5 (BOC).

The LFP apparatus was previously described.[25] Briefly, it consists of an Nd:YAG laser (Quanta Ray, GCR3-30) operating at 355 nm as the exciting source, coupled to an Applied Photophysics laser kinetic spectrometer with a Xe arc lamp as a white light source. The unfocused laser beam is directed at 90° to the sample. The laser runs at 30 Hz with individual pulses (*ca.* 5 ns) selected with a synchronised shutter. Light falling on the photomultiplier detector is sampled by a Tektronix TDS 540B oscilloscope. Transient decays are usually analysed as 35 shot averages. The samples were maintained at 295 K.

Results and discussion

When $IrI(CO)(PPh_3)_2$ **1** reacts with normal H_2 at 298 K only two signals (1 : 1) are observed in the hydride region of the corresponding ^{1}H NMR spectrum due to a pair of chemically inequivalent hydride ligands. They resonate at δ −8.5 (dt, with $^2J_{HH}$ = 4.0 Hz and $^2J_{PH}$ = 17.2 Hz) for the site *trans* to CO and δ −14.9 (dt, with $^2J_{HH}$ = 4.0 Hz and $^2J_{PH}$ = 13.8 Hz) for the site *trans* to I (Fig. 2a and b). This product is therefore readily assigned as dihydride **2**. When the same reaction is repeated with *p*-H_2 at 298 K, these two hydride resonances exhibit strong PHIP signals (SNR ∼ 700 on a 5 mg solution, SNR ∼ 280 on an optically dilute solution) and $^2J_{HH}$ is confirmed to be negative[26] (see ESI†). At 263 K, very little PHIP (SNR ∼ 2.2 on an optically dilute solution at 273 K with a single scan) is observed for the hydride resonances of **2** due to slow addition and no evidence for its minor *cis–cis* isomer was evident in ^{1}H NMR spectra even at low temperature.

When a sample of the pure dihydride $Ir(H)_2I(CO)(PPh_3)_2$ (**2**) was examined by ^{1}H NMR spectroscopy at 298 K under *p*-H_2 (3 bar), no *p*-H_2-enhanced hydride resonances were observed either with the standard PHIP protocol (45° pulse) or with the OPSY approach,[27] thereby confirming its stability with respect to H_2 loss on the time scale of these measurements. However, at temperatures of 335 K and above, PHIP-enhanced hydride resonances of **2** were observed, indicating that the thermal exchange of H_2 now becomes accessible.

In contrast to this situation, upon photo-initiation by a single laser shot at 355 nm (298 K, 3 bar *p*-H_2), the same two hydride resonances are seen with large PHIP (SNR ∼ 280) in a single scan $^1H\{^{31}P\}$ NMR measurement that is recorded after a 45° RF pulse (Fig. 2c and Scheme 1).

The nuclear spin state description of the two hydride ligands in **2***, formed after *p*-H_2 addition, reflects a longitudinal two spin order term (I_zS_z) which depends on sin 2θ (where θ is the pulse angle) and is therefore optimally encoded for detection by a 45° pulse.[9] This contrasts with the situation that was reported when the very rapid H_2 addition to $[Ru(CO)(PPh_3)_3]$ was

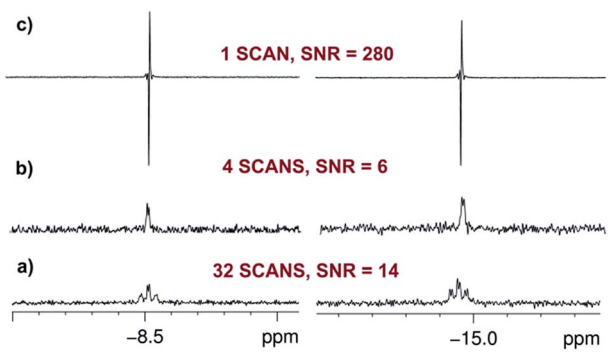

Fig. 2 Hydride region of a series of ^{1}H NMR spectra of **2** in C_6D_6 where: (a) the signals are fully relaxed prior to collection (32 scans, SNR = 14); (b) the relaxed signals are ^{31}P decoupled (4 scans, SNR = 6) and (c) the signals are hyperpolarized and ^{31}P decoupled (1 laser pulse, 1 scan, SNR = 280). The values of SNR in (b) and (c) yield an enhancement factor of 93.

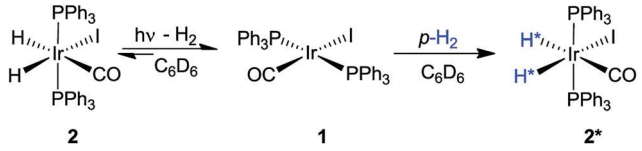

Scheme 1 Photochemical reaction to prepare **2** in a hyperpolarized state, **2***.

followed. In this latter case, the original singlet state was retained (I_zS_z + ZQ_x) and a 90° probe pulse allowed the monitoring of the evolution of the resulting zero-quantum coherences (ZQ_y).[7] This different behaviour arises because the relatively slow H_2 addition to the [IrI(CO)$(PPh_3)_2$], **1**, causes the zero quantum terms (ZQ) to lose coherence while the longitudinal two-spin order term (I_zS_z) is preserved.[8,9] The resulting I_zS_z amplitude accumulates as the reaction proceeds until all of the intermediate **1** is converted into Ir$(H)_2$I(CO)$(PPh_3)_2$ (**2**).[9]

The intensity of the hyperpolarized single scan $^1H\{^{31}P\}$ NMR signal in this photochemical experiment allows us to work with an optically dilute solution (0.7 mM in C_6D_6, $Abs_{(355)} \approx 0.7$ across the 5 mm NMR tube) whilst still obtaining a good hydride resonance signal-to-noise ratio (SNR = 280). It might be expected that this dilution ensures that a constant amount of *p*-H_2 is available in solution even if multiple observations are required. However, a control measurement showed that the detected signal intensities decreased slightly after four single laser shot experiments. We therefore refreshed the dissolved *p*-H_2 by removing the sample from the magnet/probe and re-equilibrating it with the *p*-H_2 in the headspace every four laser shots in order to ensure a reproducible response (see ESI†).

The evolution of the hydride signal intensity was followed as a function of the time, τ, between the laser pump and NMR probe steps. This corresponds to following the change in amplitude of the longitudinal two-spin order term (I_zS_z) during the pump probe delay which, in the absence of NMR relaxation, is proportional to the concentration of **2** (Scheme 1). The signal

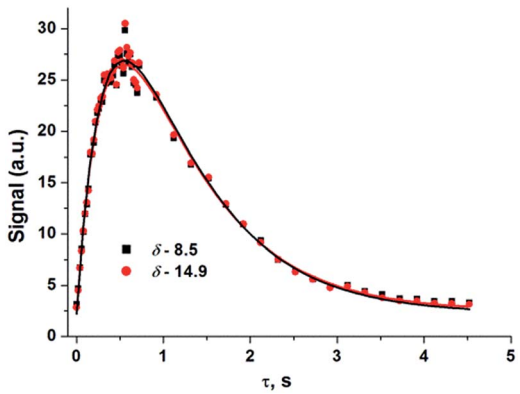

Fig. 3 Hydride signal integral values of **2*** *versus* τ (time) taken from a series of $^1H\{^{31}P\}$ NMR spectra that were recorded under 3.31 bar of *p*-H_2 pressure. Coloured squares/circles are the experimental points while the lines show the fit according to eqn (2) where R_1 has been optimised as a linked parameter in a multiple dataset fit. Points were collected in random order.

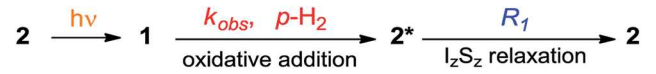

Scheme 2 Schematic diagram showing photodissociation of H_2 from **2**, oxidative addition of *p*-H_2 to **1**, and nuclear spin relaxation reactions of **2***.

versus time profile (Fig. 3) shows that an exponential growth is followed by an exponential decay which ultimately restores the initial intensity. Such a build-up and decay profile is typical of that expected for two consecutive reactions where the first product is depleted as it takes part in the subsequent one. Here, the chemical process is the formation of **2*** by *p*-H_2 addition to its photochemically formed precursor IrI(CO)$(PPh_3)_2$ **1** and proceeds with a pseudo first order-rate constant k_{obs}. The subsequent decay is due to nuclear spin-lattice relaxation of the hyperpolarized NMR signal that proceeds with the first order-rate constant R_1 (Scheme 2). These experimental data can be fitted to the function in eqn (2)[28] to yield k_{obs} of 2.1 ± 0.2 s^{-1} for H_2 oxidative addition under 3.31 bar of *p*-H_2.

$$\left(\frac{d[\mathbf{2}^*]}{dt}\right) = k_{obs}[\mathbf{2}] - R_1[\mathbf{2}^*]$$
$$[\mathbf{2}^*] = [\mathbf{2}]_0 \frac{k_{obs}}{R_1 - k_{obs}} \times \left(e^{-k_{obs}t} - e^{-R_1 t}\right) \quad (2)$$

The reformation of **2** follows pseudo-first-order kinetics under these conditions where *p*-H_2 is in excess. We therefore varied the hydrogen pressure from 3 to 6 bar to extract k_2 from the resulting series of k_{obs} values *via* the associated linear dependence analysis (Table 1 and Fig. 4).

The second order rate constant k_2, for the regeneration of **2** in the presence of hydrogen was determined from this analysis as (3.26 ± 0.42) × 10^2 M^{-1} s^{-1} (with solubility of H_2 taken as 2.9 × 10^{-3} M atm^{-1}) at 298 K.[29] In parallel to this NMR study, we also determined the kinetics of H_2 addition to **1** by transient absorption UV-vis spectroscopy§ starting from photo-excitation (355 nm) of a C_6H_6 solution of **2**. Once more, the plot of k_{obs} against H_2 pressure was linear with a corresponding second order rate constant of (3.06 ± 0.40) × 10^2 M^{-1} s^{-1}. Literature

Table 1 k_{obs} determined at different hydrogen pressures by photochemical pump-NMR probe

H_2 pressure[a] bar	Hydride at δ −8.5 k_{obs}[b], s^{-1}
3.31	2.1 ± 0.2
4.42	3.5 ± 0.4
5.10	3.7 ± 0.5
6.02	4.8 ± 0.3

[a] The amount of *p*-H_2 at 26 K was calculated as >99%.[5] [b] Polynomial fitting involved using R_1 (Scheme 2 and eqn (2)) as a shared parameter in a series of traces mapping d(**2***)/d*t* as a function of [*p*-H_2], the rate of relaxation of the double quantum term (I_zS_z) is not affected by the change in [H_2]. $1/R_1$ was determined to be 0.67 ± 0.11 s. This value was validated by measuring the rate of relaxation of the I_zS_z term independently employing a different method (See ESI)†.

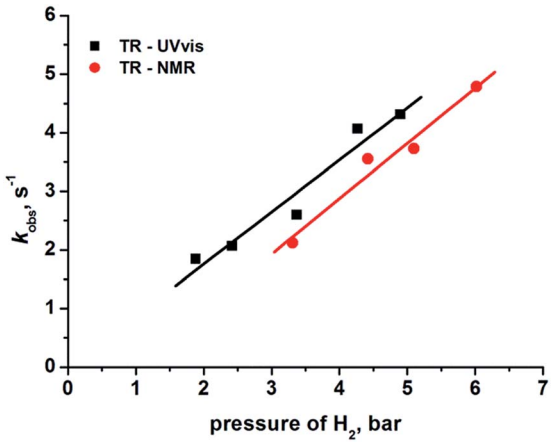

Fig. 4 Plots of pseudo-first-order rate constants k_{obs} determined from the decay of the transients obtained by TR-NMR (black squares) and TR-UV-vis (red circles) after 355 nm excitation of complex **2** in benzene *vs.* the pressure of quenching gas (H_2). The corresponding lines of best fit are shown in black and red.

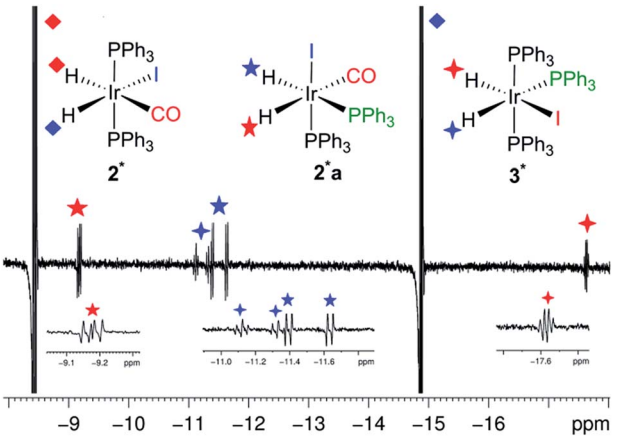

Fig. 5 Hydride region of the ^{1}H NMR spectrum of a C_6D_6 solution of 2 exposed to 32 laser shots. The major peaks belong to **2*** (diamonds); insets: same part of the spectrum magnified to observe the newly formed species **2a*** and **3***.

values for hydrogen uptake by **1** are reported as 430 M^{-1} s^{-1} in chlorobenzene and >10^2 M^{-1} s^{-1} in C_6D_6 solution at 30 °C, as determined by spectrophotometry[12] and manometry[10] techniques, respectively. These values are consistent with our TR-NMR and TR-UV-vis measurements. In Fig. 4, we use the pressure of H_2 as the *x*-axis quantity for UV/vis and NMR measurements. The underlying assumption is that **2** is formed with 100% spin-state purity. The non-zero intercept for the line through the NMR data may result from lower purity, but any such reduction has an insignificant effect on the rate k_2, because the rate is derived from the gradient of the lines.[21,30]

The effect of temperature on the reactivity of **2** towards H_2 was also tested. In order to do this, a set of similar photochemical pump-NMR probe experiments was undertaken at 315 K which gave a k_2 value of (6.0 ± 0.3) × 10^2 M^{-1} s^{-1} from the corresponding plot of k_{obs} *vs.* H_2 pressure (See ESI†); the gain in rate for this 17° increase in temperature was ~2-fold. Additionally, the rate of the same reaction was measured as a function of temperature for a C_6D_6 solution of **2** under 4.42 bar of H_2. The resulting activation parameters[31] ($\Delta H^{\ddagger}$ = 42 ± 1 kJ mol^{-1}, $\Delta S^{\ddagger}$ = −53 ± 1) (see ESI†) were consistent with the values previously reported.[10]

We also obtained further insight into the mechanism of H_2 addition to the metal centre using our pump-probe system. To clarify the mechanism, we exposed an optically dilute C_6D_6 solution of **2** under *p*-H_2 atmosphere to 48 laser shots (355 nm, repetition frequency 10 Hz, at 295 K, 3 bar *p*-H_2). The major detectable species was **2*** (Fig. 5) but by-products started to form after more than 32 laser shots. These arise from two additional photo-generated dihydride species **2a*** and **3***. The splitting of the hydride peaks and their chemical shifts indicate that both of these species contain pairs of *cis* hydrides and *cis* phosphines (Fig. 5, see ESI† for δ and J values). In **2a***, a bis phosphine complex, one hydride lies *trans* to carbonyl (δ −9.2) and the second (δ −11.5) lies *trans* to phosphorus. In **3***, one hydride ligand lies *trans* to iodine (δ −17.6) while the second (δ −11.2) is *trans* to phosphorus, but now an additional phosphorus splitting confirms its identity as the ligand exchange product $Ir(H)_2(I)(PPh_3)_3$. Their relative signal strengths are 2 and 1% of those of **2*** respectively. Photo-isomerization of square planar complexes is a well-known process.[32] We therefore propose that following the formation of **1** by reductive elimination of H_2 from **2***, secondary photolysis takes place to induce geometrical rearrangement and ligand dissociation in **1**. The resulting photo-products react promptly with *p*-H_2 giving rise to the observed enhanced signals of **2a*** and **3***. Their detection is completely suppressed by decreasing the temperature by 10° (285 K).

The identity of **3*** was also confirmed by trapping the intermediate with excess PPh_3 (see ESI†). The addition of 20 fold excess PPh_3 to an optically dilute C_6D_6 solution of **2** resulted in the observation of **3*** at room temperature after addition of *p*-H_2. The hyperpolarized hydride signals of **3*** could be made stronger by increasing the temperature to 50 °C. When the same solution was exposed to 32 laser shots, once again **2*** was the major species with **3*** being the only by-product present in solution. Under these conditions, the formation of **2a*** was prevented by the excess PPh_3 which acted as a trap for any unsaturated species formed in solution. Interestingly, the minor isomer observed by thermal reaction of the chloride analogues exhibited a *cis–cis–trans* structure that is not seen here.[23,33]

When the temperature of an optically dilute solution of **2** under *p*-H_2 was raised to 335 K, thermal exchange was observed to result in small PHIP enhancements for the hydride resonances of **2** (SNR ~ 40) in the absence of laser irradiation. In addition to these ^{1}H NMR signals, new enhanced hydride signals in the region δ −18 to −22 were detected which remained visible by PHIP for several minutes (see ESI†). These signals could also be accessed after multiple laser shots at lower temperatures (>16 laser shots at 315 K). The greater shielding of these hydride resonances is characteristic of those observed for dimers, such as $Rh(H)_2(PPh_3)_2(\mu\text{-}I)_2Rh(CO)(PPh_3)$;[20] we therefore assign these products to dimeric complexes with bridging iodine atoms (see ESI†).[20]

Conclusions

The observations that have been described here establish that the combination of *in situ* photochemistry and *p*-H_2 derived signal amplification allows the quantification of H_2 addition rates on a ms timescale by NMR spectroscopy. In this case, $IrI(CO)(PPh_3)_2$ (**1**) reacts with *p*-H_2 at room temperature to generate $Ir(H)_2I(CO)(PPh_3)_2$ (**2**) which is characterised by the PHIP-enhancement of its hydride resonances. While **2** is thermally stable to H_2 loss at 298 K, it is photoactive under 355 nm irradiation and in the presence of *p*-H_2 PHIP-enhancement is observed. Because of the signal gain associated with PHIP, the accumulation of **2** could be easily followed between 50 ms and 1 s despite the inherently low sensitivity of NMR spectroscopy. Data analysis of the kinetics of formation of **2** from **1** as a function of H_2 pressure and temperature yielded second order rate constants and activation parameters (*e.g.* $k_2 = (3.26 \pm 0.42) \times 10^2$ M^{-1} s^{-1}). This approach was validated by laser flash photolysis which yielded similar second order rate constants (*e.g.* $(3.06 \pm 0.40) \times 10^2$ M^{-1} s^{-1} at 298 K).

One benefit of this photochemical pump-NMR probe method is that we obtain high quality NMR spectra at the same time as measurement of rates of reaction, thus ensuring that we identify our products unambiguously. This method therefore contrasts with conventional laser flash photolysis where we rely on a broad UV/vis absorption of the reaction intermediate. Our *p*-H_2 approach also brings the sensitivity of NMR spectroscopy into a similar range to time-resolved UV/vis absorption spectroscopy. The nearest comparable measurements by NMR spectroscopy have been made by photo-CIDNP[34,35] or by stopped-flow NMR.[36]

Our measurements gave rate constants k_{obs} in the range 1–10 s^{-1} and second-order rate constants k_2 of *ca.* 10^3 M^{-1} s^{-1}. The evolution of the magnetic states that underpins this work has been described previously.[7,9] If this method is to be used to monitor faster reactions, it is straightforward to reduce the delays between the laser pump and the NMR probe pulses. For reactions that occur so rapidly that dephasing of the zero quantum coherence has not occurred, a more detailed analysis is required, which will be published shortly.

It should be noted that photochemical pump-NMR probe spectroscopy could also be applied in a similar manner to other reactions involving dihydrogen. However, its applicability is even more general than this because *p*-H_2 is only one of a growing number of molecules that can be prepared as a long-lived nuclear spin singlet (examples: dinitrogen, fumarate and stilbene).[37] Hence, the reactivity of many such molecules could in principle be quantified analogously by probing the time evolution of appropriate ^1H or heteronuclear NMR signals.

Acknowledgements

We are grateful to EPSRC (grant EP/K022792/1) for funding, Simon Colebrooke for helpful discussions and Dr Soumya S. Roy for the thermal measurement of the I_zS_z states lifetime in **2**.

Notes and references

‡ Data created during this research are available by request from the University of York Data Catalogue (http://dx.doi.org/10.15124 /282717d1-d7d9-428f-8b77-b98b6a8b6f80).

§ TR-UV-vis experiments were run in the presence of H_2. The use of *p*-H_2 does not change the results in this type of measurement.

1 R. Zhang and M. Newcomb, *Acc. Chem. Res.*, 2008, **41**, 468–477.
2 J. M. Butler, M. W. George, J. R. Schoonover, D. M. Dattelbaum and T. J. Meyer, *Coord. Chem. Rev.*, 2007, **251**, 492–514.
3 P. Kukura, D. W. McCamant and R. A. Mathies, *Annu. Rev. Phys. Chem.*, 2007, **58**, 461–488.
4 R. J. D. Miller, *Science*, 2014, **343**, 1108–1116.
5 R. A. Green, R. W. Adams, S. B. Duckett, R. E. Mewis, D. C. Williamson and G. G. R. Green, *Prog. Nucl. Magn. Reson. Spectrosc.*, 2012, **67**, 1–48.
6 S. B. Duckett and R. E. Mewis, *Acc. Chem. Res.*, 2012, **45**, 1247–1257.
7 O. Torres, B. Procacci, M. E. Halse, R. W. Adams, D. Blazina, S. B. Duckett, B. Eguillor, R. A. Green, R. N. Perutz and D. C. Williamson, *J. Am. Chem. Soc.*, 2014, **136**, 10124–10131.
8 C. R. Bowers and D. P. Weitekamp, *J. Am. Chem. Soc.*, 1987, **109**, 5541–5542.
9 J. Natterer and J. Bargon, *Prog. Nucl. Magn. Reson. Spectrosc.*, 1997, **31**, 293–315.
10 P. B. Chock and J. Halpern, *J. Am. Chem. Soc.*, 1966, **88**, 3511–3514.
11 L. Vaska and M. F. Werneke, *Trans. N. Y. Acad. Sci.*, 1971, **33**, 70–86.
12 L. Vaska and M. F. Werneke, *Ann. N. Y. Acad. Sci.*, 1971, **172**, 546–562.
13 A. L. Sargent and M. B. Hall, *Inorg. Chem.*, 1992, **31**, 317–321.
14 A. L. Sargent, M. B. Hall and M. F. Guest, *J. Am. Chem. Soc.*, 1992, **114**, 517–522.
15 G. L. Geoffroy, G. S. Hammond and H. B. Gray, *J. Am. Chem. Soc.*, 1975, **97**, 3933–3936.
16 L. Vaska, *Acc. Chem. Res.*, 1968, **1**, 335–344.
17 D. A. Wink and P. C. Ford, *J. Am. Chem. Soc.*, 1985, **107**, 5566–5567.
18 R. H. Schultz, *J. Organomet. Chem.*, 2003, **688**, 1–4.
19 C. J. Sleigh, S. B. Duckett and B. A. Messerle, *Chem. Commun.*, 1996, 2395–2396.
20 S. A. Colebrooke, S. B. Duckett, J. A. B. Lohman and R. Eisenberg, *Chem.–Eur. J.*, 2004, **10**, 2459–2474.
21 P. Hubler, J. Bargon and S. J. Glaser, *J. Chem. Phys.*, 2000, **113**, 2056–2059.
22 S. K. Hasnip, S. B. Duckett, C. J. Sleigh, D. R. Taylor, G. K. Barlow and M. J. Taylor, *Chem. Commun.*, 1999, 1717–1718.
23 S. K. Hasnip, S. A. Colebrooke, C. J. Sleigh, S. B. Duckett, D. R. Taylor, G. K. Barlow and M. J. Taylor, *J. Chem. Soc., Dalton Trans.*, 2002, 743–751.
24 C. E. Johnson and R. Eisenberg, *J. Am. Chem. Soc.*, 1985, **107**, 3148–3160.

25 M. C. Nicasio, R. N. Perutz and A. Tekkaya, *Organometallics*, 1998, **17**, 5557–5564.
26 C. J. Jameson, in *Multinuclear NMR*, ed. J. Mason, Plenum Press, New York, 1987, pp. 89–131.
27 J. A. Aguilar, P. I. P. Elliott, J. Lopez-Serrano, R. W. Adams and S. B. Duckett, *Chem. Commun.*, 2007, 1183–1185.
28 R. G. Wilkins, *Kinetics and Mechanism of Reactions of Transition Metal Complexes*, Wiley, VCH Weinheim, 1991.
29 M. V. Campian, R. N. Perutz, B. Procacci, R. J. Thatcher, O. Torres and A. C. Whitwood, *J. Am. Chem. Soc.*, 2012, **134**, 3480–3497.
30 D. Blazina, S. B. Duckett, T. K. Halstead, C. M. Kozak, R. J. K. Taylor, M. S. Anwar, J. A. Jones and H. A. Carteret, *Magn. Reson. Chem.*, 2005, **43**, 200–208.
31 We assume the solubility of H_2 as constant over this temperature range in a sealed system.
32 S. Thies, H. Sell, C. Schutt, C. Bornholdt, C. Nather, F. Tuczek and R. Herges, *J. Am. Chem. Soc.*, 2011, **133**, 16243–16250.
33 S. K. Hasnip, S. B. Duckett, C. J. Sleigh, D. R. Taylor, G. K. Barlow and M. J. Taylor, *Chem. Commun.*, 1999, 1717–1718.
34 A. S. Kiryutin, O. B. Morozova, L. T. Kuhn, A. V. Yurkovskaya and P. J. Hore, *J. Phys. Chem. B*, 2007, **111**, 11221–11227.
35 S. Perrier, E. Mugeniwabagara, A. Kirsch-De Mesmaeker, P. J. Hore and M. Luhmer, *J. Am. Chem. Soc.*, 2009, **131**, 12458–12465.
36 M. D. Christianson, E. H. P. Tan and C. R. Landis, *J. Am. Chem. Soc.*, 2010, **132**, 11461–11463.
37 M. H. Levitt, *Annu. Rev. Phys. Chem.*, 2012, **63**, 89–105.